

1 Type of the Paper: Article

2 Security-Constrained Optimal Dispatch of Combined 3 Natural Gas and Electricity Networks Using Genetic 4 Algorithms

5 Denis C. L. Costa^{1*}, João P. A. Vieira², Marcus V. A. Nunes³.

6 ¹ Federal Institute of Science and Technology of Pará, Ananindeua, PA, Brazil; denis.costa@ifpa.edu.br;

7 * Correspondence: email: denis.costa@ifpa.edu.br; Tel: +55 91 3278-3750

8 ² Federal University of Pará, Belém PA, Brazil. jpvieira@ufpa.br.

9 ³ Federal University of Pará, Belém PA, Brazil. mvanunes@ufpa.br.

10

11 **Abstract:** This paper proposes a method based on genetic algorithm (GA) for the security-constrained
12 optimal dispatch of integrated natural gas and electricity networks, considering operating scenarios
13 in both energy systems. The mathematical formulation of the optimization problem consists of a
14 multi-objective function which aims to minimize both cost of thermal generation (diesel and natural
15 gas) as well as the production and transportation of natural gas. The joint gas-electricity system is
16 modeled by two separate groups of nonlinear equation, which are solved by the combination of
17 Newton's method with the GA. The applicability of the proposed method is tested in the Belgian gas
18 network integrated with the IEEE 14-bus test system and a 15-node natural gas network integrated
19 with the IEEE 118-bus test system. The results demonstrate that the proposed method provides
20 efficient and secure solutions for different operating scenarios in both energy systems.

21

22 **Keywords:** Integrated Electric Power and Natural Gas Network, Optimal Power Flow, Genetic
23 Algorithm.

24

25 1. Introduction

26 In 2012, the thermoelectric power sector in Brazil generated 73.456 GWh; whereas the share of
27 natural gas increased by 50% [1]. This data provides evidence of the increasing importance of natural
28 gas in the thermal power generation of Brazil, mainly resulting from the high efficiency, low-cost
29 investment, operational flexibility and less environmental impact when compared to diesel [2]. This
30 significant increase in the installation of thermoelectric power plants using natural gas associated
31 with increased electricity demand, prompted this type of power generation to assure a greater
32 participation in electric power supply.

33 On the other hand, this fact creates a strong interdependence between the electrical system and
34 the gas pipeline system, the latter being responsible for the transportation of natural gas from the
35 production well to the consumption point. Traditionally, this interdependence is disregarded in
36 studies of optimal planning of the operation of thermoelectric power plants using natural gas.
37 However, this simplification may affect the safe operation and performance of the joint systems, as
38 pressure losses, contingencies in gas pipelines, lack of storage or interruptions in the supply of natural
39 gas may bring about a cut off of the generating units. In the occurrence of shutdowns of gas pipelines
40 or power transmission lines, inconsistent procedures for cutting off the supply of natural gas to
41 thermal electric generators may restrict the operation of the electrical system or even result in
42 additional shutdowns [3]. The active power adjustment in an arbitrary number of generators may
43 affect the flows in the gas network, which shows the interdependence between both networks [4].
44 Therefore, this strong dependence operation between these two systems requires a coordinated
45 operation to obtain reduced operating costs and congestion without jeopardize the security of power
46 systems.

47 Various models have been proposed to ensure optimal combined operation of natural gas and
48 electrical networks by means of an unified formulation. In [3], the authors performed an assessment
49 of interdependence between both networks in terms of the impact of market prices of natural gas in

50 the dispatch of the generating units. In [5], the authors presented an multiperiod generalized network
 51 flow model focusing on the economic interdependence of the combined system (electric grid, coal
 52 and natural gas). In [6], a model was presented to calculate the maximum amount of energy that
 53 should be provided to a natural gas combined cycle power plant. In [7], an integrated model of
 54 optimal dispatch was proposed to evaluate the impact of the interdependence of electricity and
 55 natural gas networks in the operational safety of the electric system. Other studies have proposed
 56 methods of optimal dispatch of joint natural gas and electric networks [8]-[12]. All these cited works
 57 used conventional optimization methods as a solution to the problem of joint gas-electricity optimal
 58 dispatch.

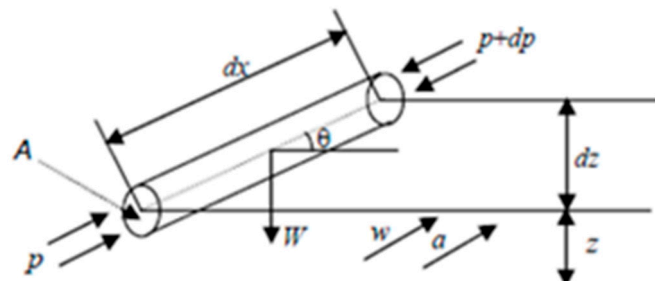
59 The electricity-gas optimal dispatch is a mixed integer, nonlinear, non-convex problem with a very
 60 complex solution. Conventional methods of nonlinear programming may not be able to provide an
 61 optimal solution taking into account that generally the solution is trapped in on local minima. As an
 62 alternative to conventional optimization methods, an evolutionary computation has been used to
 63 solve a variety of problems due to its ability to find the global optimum. However, few studies have
 64 employed evolutionary computation to solve the problem of joint electricity-gas optimal dispatch. In
 65 [13], an optimization methodology based on genetic algorithms (GA) is proposed to determine the
 66 pipeline diameter to minimize the cost of the gas network. Nonetheless, the authors did not take into account
 67 the model of the electrical grid. A hybrid model is proposed in [14], combining an
 68 evolutionary algorithm with Newton's methods and the interior points to plan for the optimal
 69 operation of the natural gas and electric systems. However, the work does not take into account the
 70 cost of transportation of natural gas in the objective function, which may reduce the overall efficiency
 71 of the system considering that the pipeline system must meet the demands for natural gas with the
 72 lowest production and transportation costs [15]-[16]. Besides, the authors of [14] did not evaluate the
 73 operating interdependence of the gas-electric system from different operational scenarios in both
 74 energy systems.

75 In this context, this paper proposes a method based on GA for security-constrained optimal
 76 dispatch of integrated natural gas and electricity networks, in order to minimize the costs associated
 77 with thermoelectric generation (natural gas and diesel), natural gas production and transportation.
 78 The nonlinear algebraic equations representing both systems are solved separately by Newton's
 79 method combined with GA in order to assess the optimal dispatch of the global energy matrix under
 80 a pre-specified operating condition.

81 The proposed method is described in detail hereinbelow in accordance with the following
 82 sections. Section II shows the formulation of the natural gas flow system considering the pipeline and
 83 the production nodes and gas consumption. section III describes the integrated electricity-gas optimal
 84 dispatch using the GA. The application of the proposed method in two coupled energy systems is
 85 presented in section IV. Finally, section V presents the conclusions of the work.

86 2. Natural Gas System Formulation

87 In order to determine the gas flow model in pipelines, it may be admitted as a reference an element
 88 of a pipeline of infinitesimal length dx (m) and transversal section A (m^2) and consider w (m/s) and a
 89 (m/s^2), respectively, the velocity and acceleration of the gas inside this element, W ($Kg.m/s^2$) weight of
 90 the gas particles, and p (bar) the external pressure as shown in Figure 1, according to [17].



91 **Figure 1.** Parameters of the gas flow in pipelines.
 92

93 Bernoulli's Equation is written as:

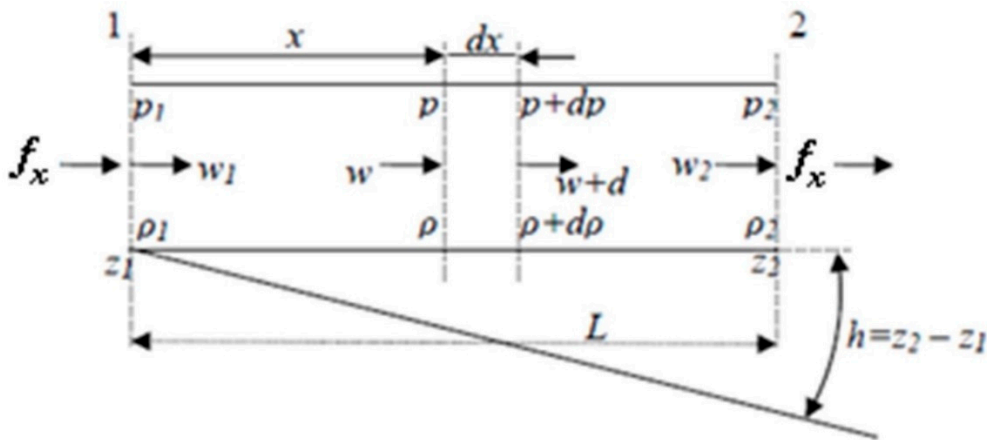
94

96

$$\frac{p}{\rho g} + \frac{w^2}{2g} + z = C$$

95

(1)



97

98

Figure 2. Gas flow in an infinitesimal portion of the pipeline.

99 In steady state, the gas flow is constant, therefore:

101

$$w_1 \cdot A_1 = w_2 \cdot A_2 = f_x$$

100

102

103 Figure 2 represents a gas flow in an infinitesimal portion of the pipeline, where:

105

104

$$w_1 \cdot \rho_1 = w_2 \cdot \rho_2$$

(2)

106

107

$$\frac{p}{\rho g} + \frac{w^2}{2g} + z = \frac{p + dp}{\rho g} + \frac{(w + dw)^2}{2g} + (z + dz) + dh_f$$

(4)

108

109

The term dh_f represents the losses in the form of heat due to friction of the gas against the pipeline wall and can be quantified by Darcy's equation.

111

$$dh_f = \frac{4f w^2}{D \cdot 2g} dx$$

110

(5)

112

113

Where f is the friction factor (dimensionless) and D is the inner diameter of the pipeline (m). By replacing (5) in (4), one has:

115

116

$$-dp = \frac{2f \rho w^2}{D} dx + \rho g dz$$

(6)

117

118

119

120

$$-pdः = \frac{2f}{D} \rho_1 p_1 w^2 dx + \frac{p^2}{p_1} \rho_1 g dz$$

(7)

The gas density is given by the inverse of the specific volume according to equation (8).

122 $\rho = \frac{1}{v}$
 121 (8)

123 The gas compressibility factor in the pipeline is given by equation (9).

125 $Z = \frac{pv}{RT}$
 124 (9)

126 From equations (7), (8) and (9), equation (10) is obtained.

127
 129 $-pdः = \frac{2f}{D} \rho_1^2 w_1^2 ZRT dx + \frac{p^2}{ZRT} gdz$
 128 (10)

130 From equations (2) and (3), equation (11) can be written as:

132 $\rho_1^2 w_1^2 = \rho_n^2 w_n^2 = \rho_n^2 \frac{f_{x(n)}^2}{A^2} = \frac{\rho_n^2 f_{x(n)}^2}{(0,25\pi D^2)^2}$
 131 (11)

133 Where the subscript *n* indicates the values for the standard pressure and temperature conditions,
 134 which are $p_n \cong 0.1MPa$ and $T_n \cong 288K$.

135 By replacing equation (11) in equation (10), equation (12) is obtained as:

137 $-pdः = \frac{32f\rho_n^2 Q_n^2}{\pi^2 D^5} ZRT dx + \frac{p_{av}^2}{ZRT} gdz$
 136 (12)

138 According to [17], $p_{av} = \frac{p_1 + p_2}{2}$ can be considered, and $p_n = \rho_n RT_n$ for gas, where as $p_n = \rho_{(ar)n} R_{ar} T_n$
 139 is for air. By dividing the two expressions for $(\rho_{ar})_n$, equation (13) can be written as:

140
 142 $\frac{\rho_n}{(\rho_{ar})_n} = \frac{R_{ar}}{R} = S$
 141 (13)

143 With *S* being the specific gravity of gas, equation (14) is obtained:

144
 146 $\rho_n = \frac{S \cdot p_n}{R_{ar} \cdot T_n}$
 145 (14)

147 By replacing equations (13) and (14) in equation (12), equation (15) can be written as:

148
 150 $-pdः = \frac{32fS ZT}{\pi^2 R_{ar} D^5} f_{x(n)}^2 \left[\frac{p_n}{T_n} \right]^2 dx + \frac{p_{av}^2 \cdot S}{Z R_{ar} \cdot T} gdz$
 149 (15)

151 By integrating equation (15) in the following intervals: $x = [0; L]$, $p = [p_1; p_2]$ and $z = h$, equation
 152 is obtained:

153
 155 $p_1^2 - p_2^2 = \frac{64f S L Z T}{\pi^2 R_{ar} D^5} f_{x(n)}^2 \left[\frac{p_n}{T_n} \right]^2 + \frac{2p_{av}^2 \cdot S}{Z R_{ar} \cdot T} gh$
 154 (16)

156 By isolating f_x , equation (17) can be written, which is the equation of gas flow according to [17].

157

$$159 f_{x(n)} = \sqrt{\frac{\pi^2 R_{ar}}{64} \cdot \frac{T_n}{p_n} \cdot \sqrt{\frac{[(p_1^2 - p_2^2) - \frac{2p_{av}^2 \cdot Sgh}{ZTR_{ar}}] \cdot D^5}{fSLZT}}} \quad (17)$$

158

160 Figure 3 shows the nodes and arcs [16] in a simplified manner. In Figure 3, Pd is the gas production
161 associated with that node, for example, Pd_g is the natural gas production at node g , $f_{x(gk)}$ is the
162 flow from one node to another; this means that f_x is the gas flow from node g to node k . Still referring
163 to Figure 3, d_{GN} are the demands for gas in each node.

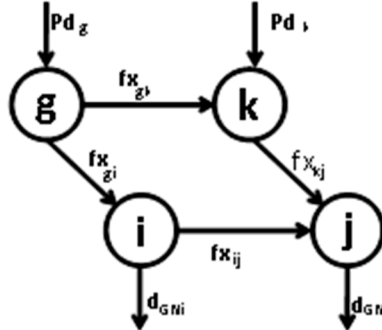
164 The supply node, which can be a gas well, a reservoir or regasification terminal of LNG (Liquefied
165 Natural Gas), may have contractual supply requirements. Depending on the flexibility of the contract,
166 the supply of natural gas may have a pre-specified range of values, a minimum (Pd_{min}) and maximum
167 (Pd_{max}) production. Mathematically:

$$169 Pd_{min} \leq Pd \leq Pd_{max}$$

170

$$171 \quad (18)$$

172



173

174

175

176

177 **Figure 3.** Simplified natural gas network.

178 For the nodes on-demand, the consumption value must always meet the demand d_{GN} .

179 In pumping gas in pipelines, there is a maximum value in the operating pressure, which refers to
180 safe pressure levels for the operation and at delivery points to consumers. Moreover, for each node
181 in the system, the gas demand should be met at a certain minimum pressure guaranteed to industries,
182 local distribution companies and thermoelectric power plants. Mathematically:

$$184 p_{min} \leq p \leq p_{max}$$

185

186

187

188 Mathematically, the flow conservation can be expressed as:

189

$$191 \sum_{j|(i,j) \in A} f_{(x)ij} = \sum_{j|(i,j) \in A} f_{(x)ji} + P_i - d_{GNI} \quad (20)$$

190

191 The gas flow through each passive pipeline $f_{(x)ij}$ is a quadratic function of the pressures at the end
192 nodes:

$$195 \text{sign}(f_{(x)ij})f_{(x)ij}^2 = C_{ij}^2(p_i^2 - p_j^2), \forall (i,j) \in A_p \quad (21)$$

194

196 The gas flow through an active pipeline is also a quadratic function of the pressures at the end nodes.
 197 In this case, the pressure at the incoming node i (or j) is lower than the pressure at the outcoming
 198 node j (or i) ($p_i < p_j$) and the gas flows from node i (or j) to node j (or i) ($f_{ij} > 0$ (or $f_{ij} > 0$)). Mathematically,

$$200 \quad C_{ij}^2 = 96,074830 \cdot 10^{-15} \frac{D_{ij}^5}{\lambda_{ij} z T L_{ij} \delta} \quad (22)$$

201
 202 Where A_p is the set of passive pipelines and A_a is the set of active pipelines and C_{ij} is a constant that
 203 depends on the length, diameter and absolute roughness of the pipeline and the gas composition as
 204 shown in (23) and (24)

$$207 \quad \text{sign}(f_{(x)ij}) f_{(x)ij}^2 \geq C_{ij}^2 (p_i^2 - p_j^2), \forall (i, j) \in A_a \quad (23)$$

$$209 \quad \frac{1}{\lambda_{ij}} = \left[2 \log \left(\frac{3,7 D_{ij}}{\epsilon} \right) \right]^2 \quad (24)$$

211 3. Combined Natural Gas and Electric Optimal Power Flow Formulation

212 The integrated gas-electricity formulation is obtained by the coupled model of power flow and
 213 natural gas flow, considering that the link between both systems is the thermal gas-fired generators
 214 which are connected to gas pipelines network.

215 The joint gas-electricity system is modeled by two separate groups of nonlinear equations, which
 216 are solved by the combination of Newton's method with the GA. Firstly, the optimal power flow is
 217 solved. Next, the gas flow is solved using the values of state variables provided by optimal power
 218 flow, in order to assess the steady-state of the overall network.

219 The attractiveness of using Newton's method is the solution with a local quadratic convergence,
 220 irrespectively of the dimension of the electric power grid, provided that all the state variables
 221 involved in the study are properly initialized. On the other hand, the solution provided by Newton's
 222 method can be trapped on local minima.

223 In the power flow solution, the voltage magnitudes are initialized 1.0 p.u. for all uncontrolled
 224 voltage bus. Meanwhile the voltage magnitudes and the active power at buses of thermal power
 225 generation (diesel and natural gas) are initialized by GA at specified values that remain constant
 226 throughout the iterative solution provided by the Newton-Raphson method. The active power of the
 227 slack generator is not initialized by GA, considering that this slack bus is responsible for supplying
 228 the entire imbalance of active power in the system, even when a sufficient spinning reserve exists on
 229 other generators.

230 The strategy adopted for the gas flow solution is similar to that of the load flow. The initial nodal
 231 pressures at the pipelines are measured in Baria. The initial values of pressures and gas flow in
 232 producing nodes are provided by GA, remaining constant throughout the iterative solution process
 233 provided by Newton's method. As for the power flow solution, the gas to be produced by the swing
 234 node is not initialized by GA. It is repeated while the maximum generation's number hasn't been
 235 reached. Therefore, the proposed approach fully takes the advantages of both evolutionary strategy
 236 optimization and classical method in the attempt to jump out from the local optimal point. It increases
 237 the precision and quickens the convergence. The flowchart of this approach is depicted in Figure 4.

238 The scope of this article is to propose a method of joint electricity-gas optimal dispatch, under
 239 security constraints that aims to minimize the total operating cost of the gas-electricity system.
 240 Thus, the formulated objective function is represented by:

$$243 \quad \text{Min} \sum C_g \cdot PG + \sum C_T \cdot f_x + \sum (a + b \cdot P_{ger} + c \cdot P_{ger}^2) \quad (25)$$

245 Subject to:

$$247 \quad \sum_{j|(i,i) \in A} f_{(x)ij} = \sum_{j|(j,i) \in A} f_{(x)ji} + Pd_i - d_{GNi}$$

$$sign(f_{(x)ij})f_{(x)ij}^2 = C_{ij}^2(p_i^2 - p_j^2), \forall (i,j) \in A_p$$

$$sign(f_{(x)ij})f_{(x)ij}^2 \geq C_{ij}^2(p_i^2 - p_j^2), \forall (i,j) \in A_a$$

$$Pd_{\min} \leq Pd \leq Pd_{\max}$$

$$253 \quad \quad \quad 256 \quad \quad \quad n_1 \leq n \leq n_2$$

$$P_{\mathcal{C}_i} = Re(\Psi_i(V, \theta)) = P_{\mathcal{C}_i} \forall i \in N_{\mathcal{C}}$$

$$258 \quad \theta_{i+1} = \text{Im}(\psi(V, \theta_i)) = \theta_i \quad \forall i \in N$$

$$259$$

239 $Q_{Gi} - Im(\varphi_i(v, \theta)) = Q_{Li}; \forall i \in N_B$
 260

$$261 \qquad \qquad \qquad V_{i,min} \leq V_i \leq V_{i,max}; \; \forall i \in N_B$$

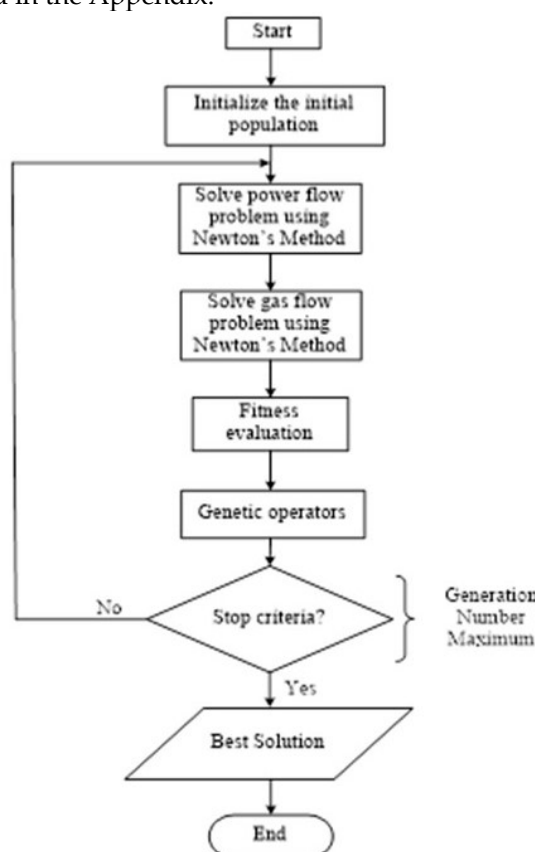
$$263 \qquad \qquad \qquad |P_{ij}(V, \theta)| \leq P_{ij,max}; \forall i \in N_B$$

$$P_{Gi,min} \leq P_{Gi} \leq P_{Gi,max}; \forall i \in N$$

$$Q_{Gi\ min} \leq Q_{Gi} \leq Q_{Gi\ max}; \forall i \in N_G$$

268

270 The variables are described in the Appendix.



271

Figure 4. Flowchart of the proposed method

273

274 4. Case Studies

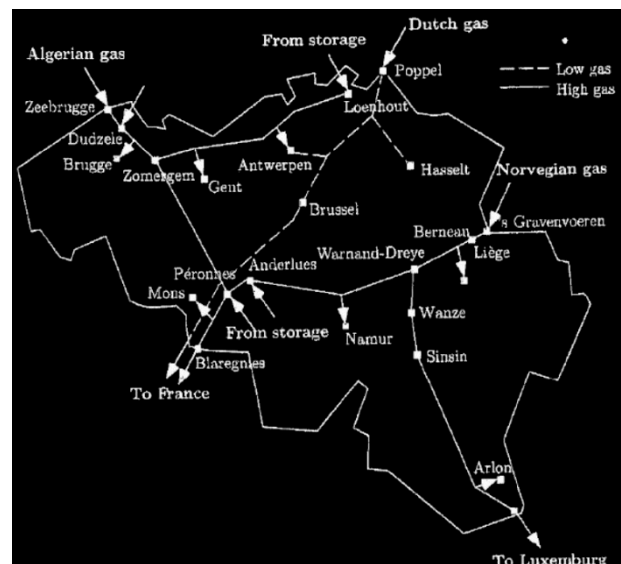
275 The proposed method for optimal dispatch of the power grid combined with the natural gas
 276 network is tested in two systems, namely:

277 • Case 1: The Belgian natural gas network integrated to the IEEE 14-bus electric grid;
 278 • Case 2: 15-node natural gas network integrated to the IEEE 118-bus electrical grid.

279

280 a) Case 1

281 The proposed method is applied to determine the optimal gas-electricity operation made up by
 282 the Belgian natural gas network [16], shown in Fig. 5, and the IEEE 14-bus electric grid [18], illustrated
 283 in Fig. 6. The 20-node Belgian natural gas network consists of eight nodes for gas consumption for
 284 non-electrical purposes, seven nodes for gas production and 24 pipelines [16]. The node referred to
 285 as Zeebugge is considered the slack node. On the other hand, the electric grid is assumed to consist
 286 of two natural gas generators connected to bus bars 2 and 3, which are supplied by nodes 4
 287 (Zomergen) and 12 (Namur) of the natural gas network, respectively. For analysis purposes, the
 288 optimal gas-electricity solution was obtained assuming the following operating conditions in both
 289 systems: (a) base case; (b) shutdown of the pipeline between nodes 4 and 14; (c) 20% increase in the
 290 total gas demand for non-electric purposes; and (d) 20% increase in the total load of the electrical
 291 grid.



292

293 **Figure 5.** Belgian natural gas network.

294

295

296

297

298

299

300

301

302

303

304

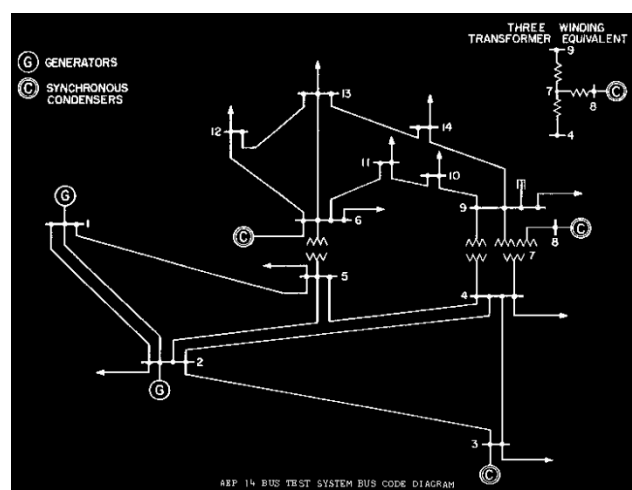
305

306

307

308

309

310 **Figure 6.** IEEE 14-bus network.

310 Table 1 shows the correspondence between the nodes of the Belgian natural gas network and the
 311 cities to the Figure 5.

312
 313 **Table 1.** Nodes and Cities- Belgian Natural Gas Network

314 Node	City	315 Node	City	316 Node	City	317 Node	City
1	Zeebrugge	6	Antwerpen	11	Warnand	16	Blaregnes
2	Dudzele	7	Gent	12	Namour	17	Wanse
3	Brugge	8	Voeren	13	Anderlues	18	Sinsin
4	Zomergem	9	Berneau	14	Péronnes	19	Arlon
5	Loenhout	10	Liège	15	Mons	20	Luxemburg

320
 321 Table 2 shows the coefficients for the costs of thermal power generation using natural gas
 322 (connected to bus bars 2 and 3) and diesel (connected to the buses 1 and 4) of the 14-bus electric grid.
 323 Figures 7, 8 and 9 show the results of the joint electricity-gas optimal dispatch with power provided
 324 by natural gas and diesel-fired generators, the natural gas flows and nodal pressures of the gas
 325 network, respectively. Table 3 presents the total costs of the integrated electricity-gas optimal
 326 dispatch with the cost of thermoelectric power generation (gas and diesel) and the production and
 327 transportation costs of natural gas. The results presented are related to the operating conditions: (a),
 328 (b), (c) and (d).

329 All generators have regulated their active powers to meet the economic criteria, according to the
 330 operation scenario without compromising the security of the gas-electricity system. The voltages in
 331 the buses of the electric system, the thermal capacity of lines and transformers and reactive capacity
 332 of the generators were not violated.

333
 334 **Table 2.** Operational Characteristics of Gas- and Diesel-Fired Generators

335 Unit	Cost coefficients (\$/MWh)			P _{G,min} (MW)	P _{G,max} (MW)
	a1	b1	c1		
1	2239	21.02	0.009	10	150
4	1469	19.71	0.077	10	100

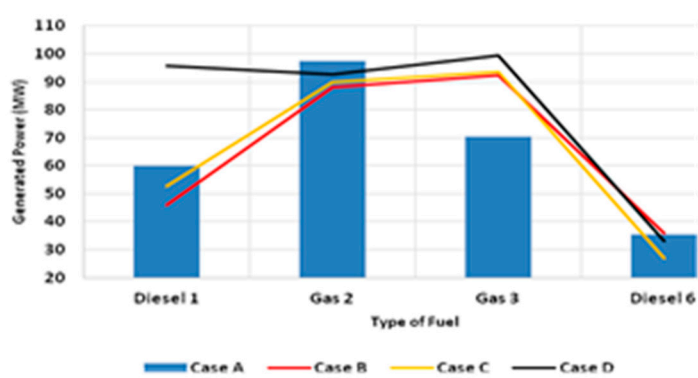
336 Tower (node)	337 Unit	Gas supply coefficients (Mm ³ /Mw)			P _{G,min} (MW)	P _{G,max} (MW)
		K ₀	K ₁	K ₂		
Zomerge n (4)	2	0.00	0.005	0.00	0	100
Namur (12)	3	0.00	0.005	0.00	0	100

338 Figure 7 shows that natural gas-fired generators injected a greater amount of active power
 339 compared to diesel generators for the base case (a), showing the efficiency of the method to minimize
 340 the cost of thermal power generation (natural gas and diesel). For cases (b) and (c), which correspond
 341 to different scenarios of the gas network in relation to the base case, figure 7 illustrates that natural
 342 gas-fired generators also injected more active power when compared to diesel-fired generators.

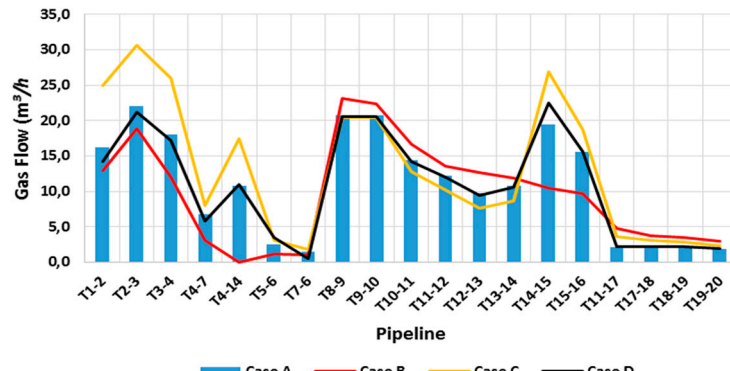
343 The model adopted first solves the optimal power flow through Newton's method combined with
 344 GA, and subsequently solves for the gas flow also by Newton's method combined with GA. In other
 345 words, in case there are no changes in the scenarios in the electric grid, the results to be obtained for
 the optimal dispatch of thermal units tend to be very close. These similar results take into account

346 that the GA has associated structures to the probability. For this reason, the generation levels obtained
 347 for cases (b) and (c) are close to those in case (a). On the other hand, cases (b) and (c) could have been
 348 critical considering that both the shutdown of a pipeline and the increase of gas consumption for non-
 349 electrical purposes could have restricted the supply of natural gas to generating units. However, the
 350 solution of the gas flow converged to cases (b) and (c), ensuring the supply of natural gas to nodes 4
 351 and 14, which in turn correspond to the nodes that supply the gas-fired generators. It is important to
 352 note that producing nodes store gas for supply in scenarios of increased natural gas demand. For case
 353 (d) both the diesel and gas-fired generators contribute with the increase in electric demand.

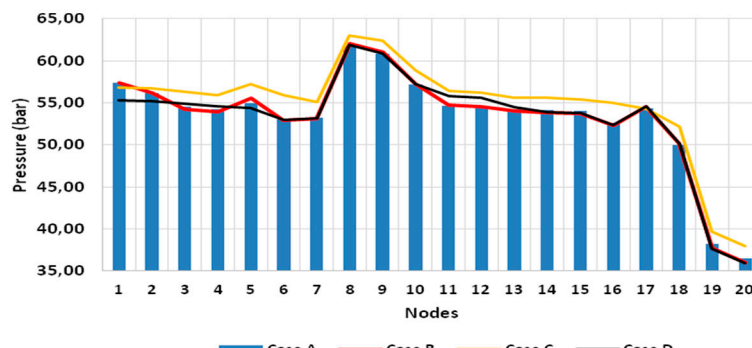
354 Figures 8 and 9 illustrate the flow in the pipeline network and the pressures at each node of the
 355 network, respectively. It is possible to notice in case (b) an interruption of the gas flow in the branch
 356 between nodes 4 and 14. Such contingency causes a reduction in gas production illustrated in Fig. 10
 357 in nodes 1, 2 and 5, reducing the flow in the pipelines located in the upper part of the gas system.
 358 Since node 14 does not receive gas from node 4, gas production in nodes 8, 13 and 14 increases to
 359 maintain the systems supplied.



371 **Figure 7.** Optimal dispatch of diesel and gas-fired generators [MW].



384 **Figure 8.** Natural gas flows at pipelines [m³/h].

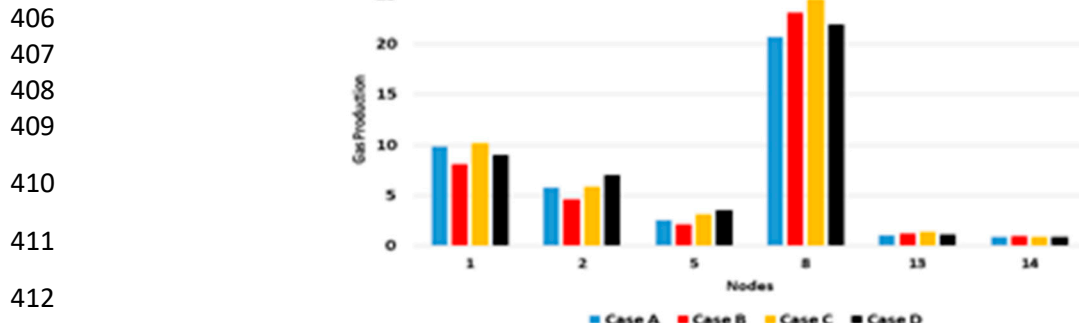


397 **Figure 9.** Nodal pressures [bar].

398 Case (c) reflects an increase in the demand for gas for non-electrical purposes. This condition
 399 causes an increase in gas supply and an increased gas flow transported in pipelines and the pressures
 400 of the nodes, as can be observed in Figures 8 and 9. For the scenario applied in case (d), which refers
 401 to an increased electrical power demand, it can be observed in Figs. 8 and 9 that the branches
 402 responsible for supplying nodes 4 and 12 (nodes that supply the thermal gas-fired generators)
 403 undergo an increase in gas flow without a significant pressure variation in the nodes.

404

405



412

413

Figure 10. Gas Production [Mm³].

414

415 The scenario presented in Case (b) simulates an interruption in the pipeline between the cities of
 416 Zommergen (node 4) and Perrones (node 14). This contingency causes a division of the gas network
 417 in two systems, generating an islanding pipeline. So producers nodes located in the cities of
 418 Zeebrugge (node 1), Dudzele (node 2) and Lorenhout (node 5) decrease the level of natural gas
 419 production, as shown in Figure 10. Consequently, the gas flow in the branches 1-2, 2-3, 3-4, 5-6, 6-7
 420 and 7-4 reduces in the same proportion in accordance with Figure 8, since there isn't a demand gas
 421 from node 4 to node 14.

422

423 In the lower portion of the gas system an inverse process occurs. Without the amount of gas
 424 transported from node 4 to 14, the producers nodes located in the cities of Voeren (node 8), Anderlues
 425 (node 13) and Perrones (node 14) increase their level of gas production (Figure 10), causing an
 426 increase in the gas flow in that part of the pipeline network (Figure 8). Thus, the Genetic Algorithm
 427 (AG) evaluate the levels of security of electric and gas system and optimizes the solution to new
 428 values of the costs, as shown in case (b) of the Table 3 below.

429

430 This scenario demonstrates the importance of the security-constrained studies related with
 431 integration of gas network and electric systems. At the same time it's possible to guarantee the
 432 process of cost optimization (minimization of costs) based on GA as described previously.

433

434 Table 3 depicts the operating costs for each scenario. It is observed that the costs are subject to
 435 individual variations due to the contingency brought about in the respective simulation. The largest
 436 identified cost refers to the increase in electricity demand, represented by scenario (d).

437

438

439

440

441

442

443

444

Table 3. Optimal Dispatch Costs

Scenarios	Case A	Case B	Case C	Case D
Generation cost	5365,50	5,371.82	5,351.17	6,654.60
Gas production cost	2880,20	2905.00	2,991.40	3,032.76
Gas transport cost	709,83	763.20	819.77	777.67
Gas total cost	3590,00	3,668.20	3,811.17	3,810.43
Total cost	8955,50	9,040.02	9,322.37	10,465.03

445

446

447

448

449

450

451

452

453

454

455

456

457

458

459

460

461

462

463

464

465

466

467

468

469

470

471

472

473

474

475

476

477

478

479

480

481

482

483

484

485

486

487

488

489

490

491

492

493

494

495

496

497

498

499

500

501

502

503

504

505

506

507

508

509

510

511

512

513

514

515

516

517

518

519

520

521

522

523

524

525

526

527

528

529

530

531

532

533

534

535

536

537

538

539

540

541

542

543

544

545

546

547

548

549

550

551

552

553

554

555

556

557

558

559

560

561

562

563

564

565

566

567

568

569

570

571

572

573

574

575

576

577

578

579

580

581

582

583

584

585

586

587

588

589

590

591

592

593

594

595

596

597

598

599

600

601

602

603

604

605

606

607

608

609

610

611

612

613

614

615

616

617

618

619

620

621

622

623

624

625

626

627

628

629

630

631

632

633

634

635

636

637

638

639

640

641

642

643

644

645

646

647

648

649

650

651

652

653

654

655

656

657

658

659

660

661

662

663

664

665

666

667

668

669

670

671

672

673

674

675

676

677

678

679

680

681

682

683

684

685

686

687

688

689

690

691

692

693

694

695

696

697

698

699

700

701

702

703

704

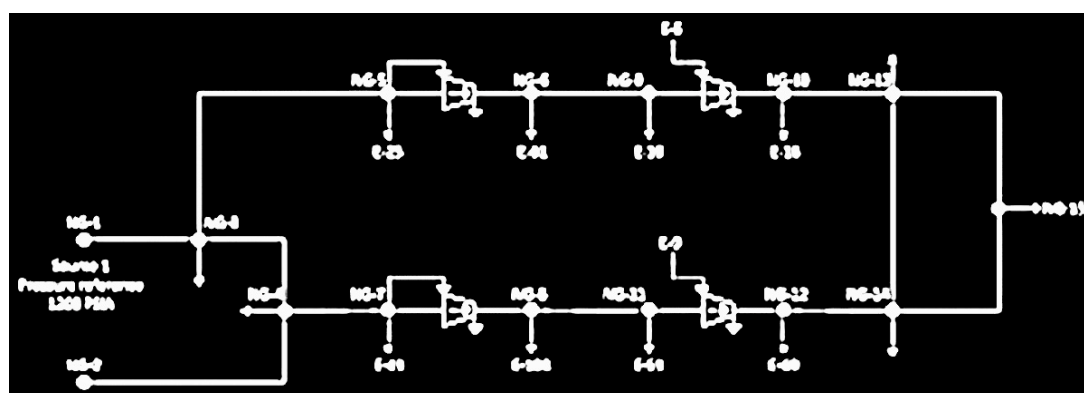
705

445 its optimal value. The 2nd situation is related to disruption in the gas flow in a branch of 55 miles
 446 long.

447 *b) Case 2*

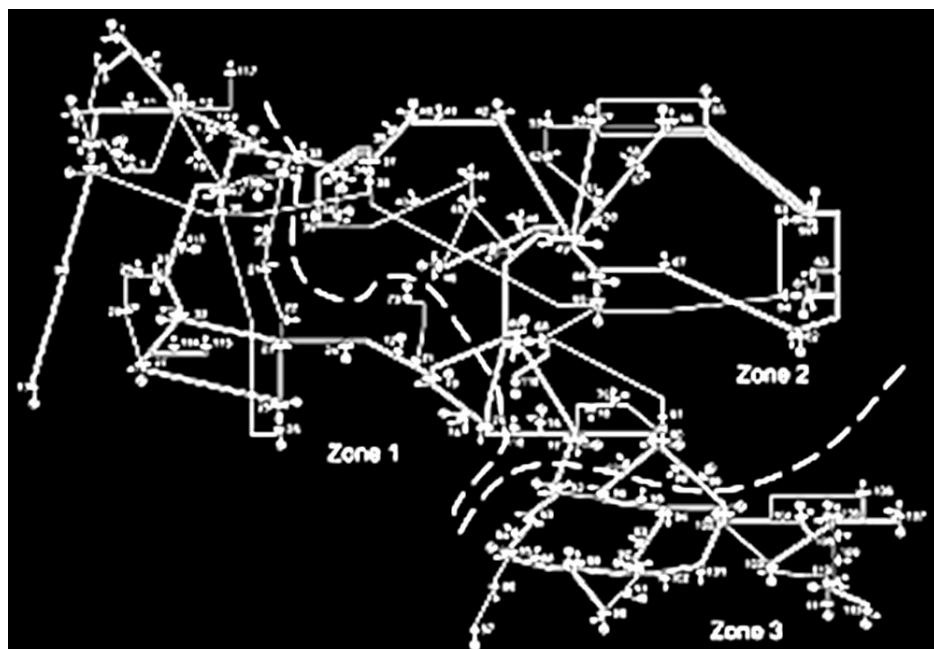
448 The proposed method is also applied to obtain the optimal dispatch of the electricity-gas system
 449 made up of the 15-node natural gas network [8], shown in Figure 11, and the IEEE 118-bus electric
 450 grid [18], shown in Figure 12. The 15-node natural gas network consists of five nodes for the
 451 consumption of gas for non-electrical purposes, and two nodes for gas production, and 16 gas
 452 pipelines. Node 1, is considered the slack node. Table 4 shows the operational characteristics of these
 453 networks.

454 On the other hand, the 118-bus electric grid is assumed to be made up of 118 buses for nineteen
 455 generators, out of which 8 gas-fired generators and 11 diesel-fired generators. For analysis purposes,
 456 the optimal gas-electricity solution was obtained assuming the operating conditions in both
 457 networks: (a) base case; (b) shutdown of two gas pipelines between nodes 3 and 4 and another
 458 between nodes 13 and 14; (c) 20% increase in the total gas demand for non-electric purposes; and (d)
 459 a 20% increase in the total power of the electric grid.



460
 461
 462
 463

Figure 11. 15-node natural gas network.



464
 465
 466
 467

Figure 12. IEEE 118-bus network.

468

Table 4. Operational Characteristics of Gas and Diesel-Fired Generators

Unit	Cost coefficients (\$/MWh)			P _{G,min} (MW)	P _{G,max} (MW)
	a1	b1	c1		
26, 31, 46, 54, 65, 66	2239	21.02	0.009	10	150
69, 80, 87, 100, 111	1469	19.71	0.077	10	100

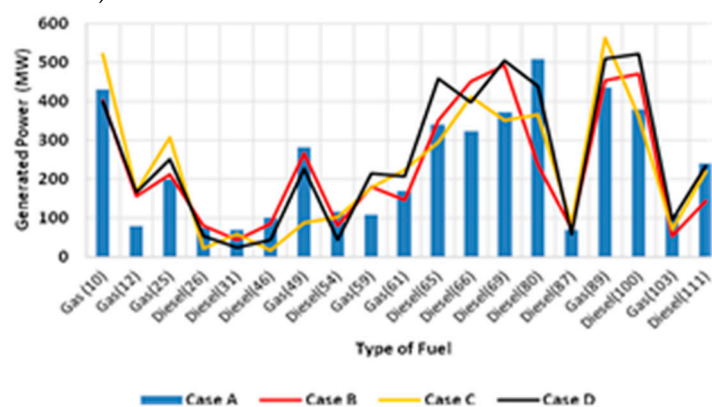
469

Node	Unit	Gas supply coefficients (Mm ³ /Mw)			P _{G,min} (MW)	P _{G,max} (MW)
		K ₀	K ₁	K ₂		
5, 6, 7, 8	10, 12, 25, 49	0.00	0.005	0.00	0	100
9, 10, 11, 12	59, 61, 89, 103	0.00	0.005	0.00	0	100

470

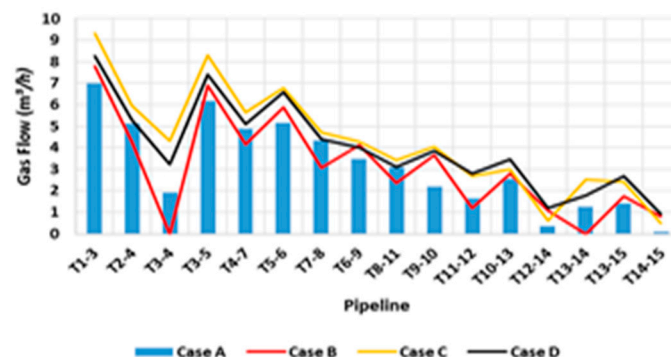
471 Figures 13, 14 and 15 show the results of integrated gas-electricity optimal dispatch with the
 472 powers provided by natural gas and diesel generators, the natural gas flows, and the nodal pressures
 473 of the gas network, respectively. Table 5 presents the total costs of integrated gas-electricity optimal
 474 dispatch with the cost of thermoelectric power generation (gas and diesel) and the costs for the
 475 production and transportation of natural gas. The results presented are related to the operating
 476 conditions: (a), (b), (c) and (d).

477 As can be observed in Figure 13, all generators regulate their active powers to meet the economic
 478 criteria according to the operation scenario without compromising the security of the gas-electricity
 479 system. Figure 13 shows that natural gas-fired generators connected to buses 10 and 89, respectively,
 480 injected a greater amount of active power compared to the other generators in the system to the base
 481 case (a), showing the efficiency of the method to minimize the cost of thermoelectric power
 482 generation (gas and diesel).

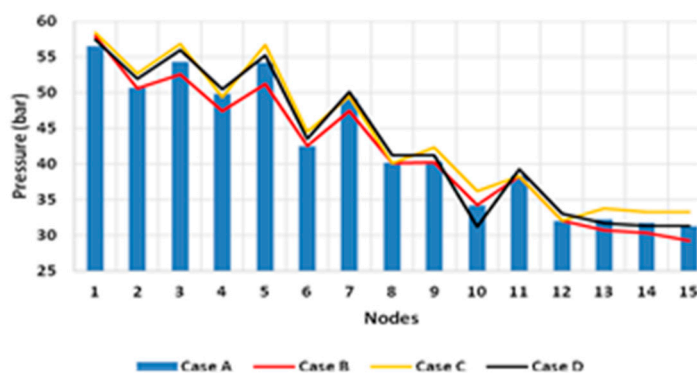
**Figure 13.** Optimal dispatch of diesel and gas-fired generators [MW].

496

497 It's noted that contingency in the pipelines between the nodes 3→4 and 13→14, represented by
 498 the case (b), causes an increase in the cost of gas production and a reduction in cost of transportation.
 499 Again the 1st situation is explained by the need of the node 2 produce a quantity of gas higher than
 500 its optimal value. The 2nd situation is related to disruption in the gas flow in the branches cited above,
 501 as shown in Figure 14.



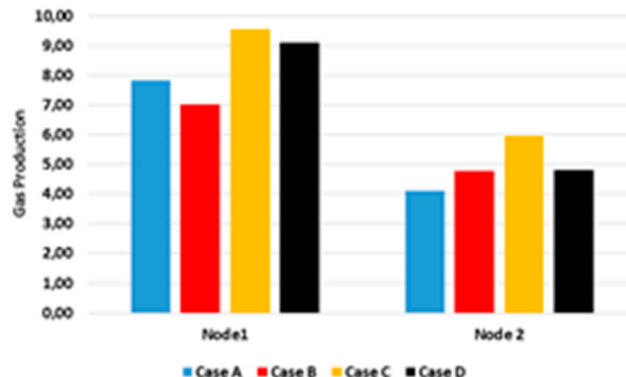
502
 503
 504
 505
 506
 507
 508
 509
 510
 511
 512
 513
Figure 14. Natural gas flows in pipelines [m³/h].



514
 515
 516
 517
 518
 519
 520
 521
 522
 523
 524
 525
 526
 527
Figure 15. Nodal pressures [bar].

528
 529
 530 As expected, case c) returns an increase in gas flow transported in pipelines, the pressures of the
 531 nodes and in gas production, as can be observed in Figures 14, 15 and 16 respectively.

532 Table 5 shows the operating costs for the scenarios presented herein. It is verified that the costs
 533 are subject to individual variations due to the contingency brought about in the respective simulation.
 534 Similar to case 1, the largest identified cost refers to the increase in electricity demand, represented
 535 by scenario (d), because this scenario reflects an increase in the generation of electricity in diesel-fired
 536 power plants.



537
 538
 539
 540
 541
 542
 543
 544
 545
 546
 547
Figure 16. Gas Production [Mm³].

549
550**Table 5:** Optimal Dispatch Costs

Scenarios	Case A	Case B	Case C	Case D
Generation cost	136,344.23	137,025.77	136,437.12	228,560.00
Gas production cost	10,277.05	10,538.00	12,129.00	11,278.00
Gas transport cost	1,461.63	1,406.00	1,855.40	1,739.90
Gas total cost	11,738.68	11,944.00	13,984.40	13,017.90
Total cost	148,082.91	148,969.77	150,421.52	241,577.90

551
552
553
554
555

558 5. Conclusions

559 This paper proposes a genetic algorithm-based optimal dispatch method of integrated gas-
560 electricity networks, considering operating scenarios. A mathematical model of this problem was
561 formulated as an optimization problem where the objective function is to minimize both cost of
562 thermal generation (diesel and natural gas) as well as the production and transportation of natural
563 gas subject to electric system and natural gas pipeline constraints.

564 The integrated electricity-gas optimal power flow problem is solved using a hybrid approach
565 which combines genetic algorithm with Newton's method. The tests on the Belgian gas network
566 integrated with the IEEE 14-bus test system and the 15-node natural gas network integrated with the
567 IEEE 118-bus test system demonstrate the effectiveness of the proposed optimal dispatch approach
568 taken into account Gas transportation cost and security-constrained which were guaranteed even in
569 contingencies conditions of the gas system and demand variable as demonstrated in both cases.

570
571

572 Appendix

573 C_g - electricity generation cost;
574 C_T - natural gas transportation cost;
575 PG -active power generated;
576 P_{ger} - Active power from gas and diesel-fired generators;
577 N_B - bus number;
578 N_G - generators number;
579 Ψ_i - complex power injection;
580 P_{Gi}, P_{Li} - active power generated and demand at bus i;
581 Q_{Gi}, Q_{Li} - reactive power generated and demand at bus i ;
582 $V_{i,\min}, V_{i,\max}$ - voltage limits;
583 V, θ - Voltage Magnitude and angle of electric bus;
584 P_{ij} - Active power between bus i e j;
585 $P_{ij,\max}$ - active power limitation in line ij;
586 $Q_{Gi,\min}; Q_{Gi,\max}$ - reactive power limits.

587
588
589

References

590 [1] MME, Ministry of Mines and Energy, 2012. [Online]. Available: <http://www.mme.gov.br>

591 [2] S. M. Kaplan, "Displacing coal with generation from existing natural gas-fired power plants,"
592 CRS Report for Congress, 7-5700, R41027, Jan. 19th, 2010 [Online]. Available:
593 <http://assets.opencrs.com/rpts>

594 [3] M. Shahidehpour, Y. Fu, and T. Wiedman, "Impact of natural gas infrastructure on electric
595 power systems," *Proc. IEEE*, vol. 93, no. 5, pp. 1042–1056, May 2005.

596 [4] A. M. Mares and C. R. F. Esquivel, "A unified gas and power flow analysis in natural gas and
597 electricity coupled networks", *IEEE Trans. Power Syst.*, vol. 27, no. 4, pp. 2156–2166, Nov. 2012.

598 [5] A. Quelhas, E. Gil, J. D. McCalley, and S. M. Ryan, "A multiperiod generalized network flow
599 model of the U.S. integrated energy system: Part I—Model description," *IEEE Trans. Power Syst.*,
600 vol. 22, no. 2,
601 pp. 829–836, May 2007.

602 [6] J. Munoz, N. Jimenez-Redondo, J. Perez-Ruiz, and J. Barquin, "Natural gas network modeling
603 for power systems reliability studies," in *Proc. IEEE/PES General Meeting*, Jun. 2003, vol. 4, pp. 23–
604 26.

605 [7] L. Tao, M. Eremia and Shahidehpour "Interdependency of natural gas network and power
606 systems security", *IEEE Trans. Power Syst.*, vol. 23, no. 4, pp. 1817–1824, Nov. 2008.

607 [8] S. An, Q. Li, and T. W. Gedra, "Natural gas and electricity optimal power flow," in *Proc.*
608 *IEEE/PES Transmission and Distribution Conf. Expo.*, 2003, vol. 1, pp. 7–12.

609 [9] C. Liu, M. Shahidehpour, Y. Fu, and Z. Li, "Security-constrained unit commitment with
610 natural gas transmission constraints," *IEEE Trans. Power Syst.*, vol. 24, no. 3, pp. 1523–1536, Aug.
611 2009.

612 [10] Arnold, M. & Andersson, G. "Decomposed electricity and natural gas optimal power flow",
613 Proceedings of 16th Power Systems Computation Conf. (PSCC), Glasgow, Scotland, Jul. 2008.

614 [11] Chaudry, M.; Jenkins, N. & Strbac, G. "Multi-time period combined gas and electricity network
615 optimisation", *Elec. Power Syst. Research*, Vol. 78, No. 7, pp. 1265-1279. 2008.

616 [12] Geidl, M. & Andersson, G., "Optimal power flow of multiple energy carriers", *IEEE Trans. Power*
617 *Syst.*, Vol. 22, No. 1, pp. 145-155. 2007.

618 [13] O. F. M. El-Mahdy, M. E. H. Ahmed and S. Metwalli, "Computer aided optimization of natural
619 gás pipe networks using genetic algorithm" *Applied Soft Computing*, Vol 10, no 4, Sep 2010, pp.
620 1141-1150.

621 [14] C. Unsiuay, J. W. Marangon Lima, and A. C. Zambroni de Souza, "Modeling the integrated
622 natural gas and electricity optimal power flow," in *Proc. IEEE/PES General Meeting*, Jun. 2007, pp.
623 24–28.

624 [15] D. Wolf and Y. Smeers, "Optimal dimensioning of pipe networks with application to gas
625 transmission networks", *Operations Research*, vol. 44, no. 4, Jul/Ago 1996, pp. 596-608.

626 [16] D. Wolf and Y. Smeers, "The Gas transmission problem solved by an extension of the simplex
627 algorithm", *Management Science*, vol. 46, no. 11, November 2000, pp. 1454-1465.

628 [17] A. J. Osiadacz, *Simulation and analysis of gas networks*, London: E. & F. N. Spon, 1987, pp. 273.

629 [18] [Online]. Available: <http://www.ee.washington.edu/research/pstca/>.

630

631

632